Demonstration of a silicon nitride optical beamforming network based on Blass-matrix architecture

E. Loukisa[1], E. Andrianopoulos[1], A. Raptakis[1], G. Megas[1], D. Gounaridis[1], A. Grammatikaki[1], R.B. Timens[3], P. van Dijk[3], L. Gounaridis[1], P. Groumas[1,2], C. Tsokos[1], Ch. Kouloumentas[1,2], H. Avramopoulos[1], C.G.H. Roeloffzen[3]

[1]School of Electrical & Computer Engineering, National Technical University of Athens, Greece
[2]Optagon Photonics, Ag. Paraskevi 15341, Athens, Greece
[3]LioniX International BV, AL 7500 Enschede, The Netherlands

Abstract: System evaluation of a silicon-nitride-integrated 4x4 Blass-matrix optical beamformer, demonstrating the first-ever error-free single-beam operation at frequencies up to 12 GHz with 1 Gbaud QPSK modulated signals across 30°–150° beam angles. © 2024 The Author(s)

1. Introduction

Beamforming plays a key role in modern communication and radar systems by significantly enhancing signal directionality, improving data transmission efficiency, and increasing detection accuracy. Through energy concentration in specific directions, beamforming maximizes signal strength while minimizing interference, enabling more efficient spectrum usage in applications such as satellite communications, 5G and beyond networks [1]. Optical beamforming, which leveraged optical methods to process the microwave signal in the optical domain rather than in the microwave domain, offers superior precision and bandwidth by providing fine control over signal phase and amplitude whilst reducing hardware complexity, facilitating the development of compact and lightweight systems.

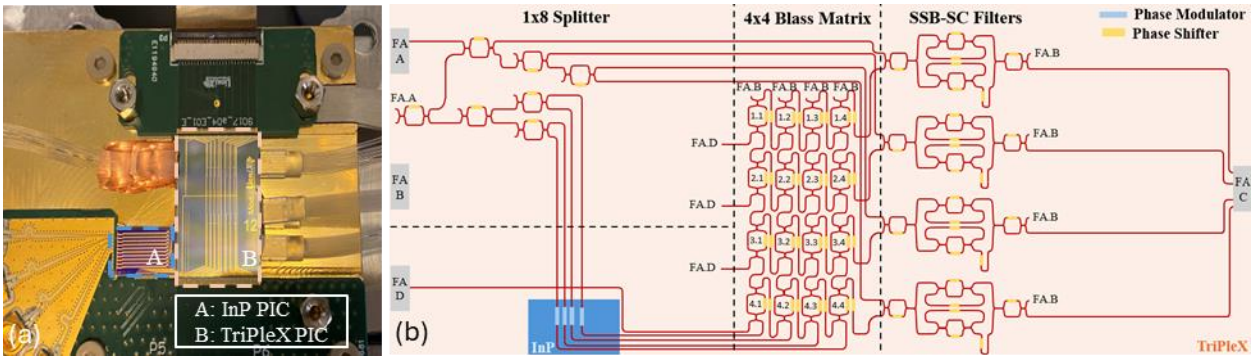

Fig. 1. (a) Picture of the 4x4 OBFN PIC comprising of an InP PIC (blue dashed lines) and a TriPleX® PIC (orange dashed lines). (b) High-level functional layout of the integrated PIC.

There are two types of OBFNs: those based on true-time delay (TTD) elements [2,3], and those using phase shifters [4], each with distinct pros and cons. TTD-OBFNs offer precise, frequency-independent delays, making them well suited for broadband systems. However, their implementation is complex and doesn't scale gracefully. In contrast, OBFNs based on phase shifters are simpler, facilitating their scaling to large number of wireless beams and antenna elements. In the context of phase shifter-based OBFNs, architectures based on Butler [5], Nolen [6], and Blass [7], matrices have been proposed, mimicking their microwave counterparts. Among these architectures, the Blass matrix is the only one guaranteeing fully flexible selection of beam angles, making it particularly suited for dynamic beam steering applications. Recently, a hybrid integrated 3x12 Blass-matrix-based OBFN has been demonstrated on InP and silicon nitride platforms [4]. The photonic integrated circuit (PIC) has been developed for use in a synthetic aperture radar receiver, with its performance evaluated using unmodulated sine waves at 9.65 GHz. A 4x4 OBFN integrated on the silicon-nitride platform, resembling a Blass-matrix architecture has been also reported, for operation at 27.5 GHz but only limited to unmodulated sine waves [8]. The architecture is based on TTD elements in the form of passive waveguides rather than phase shifters, which inherently define specific beam directions.

In this work, we report on the first-ever experimental performance evaluation of an integrated 4x4 OBFN, based on the Blass-matrix architecture with modulated microwave signals. As shown in Fig. 1. (a) the OBFN-PIC consists of the silicon-nitride platform from LioniX Int., known as TriPleX®, hybridly integrated by means of edge-coupling with the InP platform from Fraunhofer Heinrich Hertz Institute. We utilized quadrature phase-shift keying (QPSK) modulated signals at baud rates of 0.25, 0.5 and 1 Gbaud, with central frequencies at 10 and 12 GHz. An experimental

setup was developed to emulate the OBFN-PIC's operation in the downlink direction of a wireless communication system. The performance was evaluated based on the error vector magnitude (EVM) of the decoded signals for beam angles ranging from 30° to 150°. In all instances, we achieved error-free performance, validating the capability to form and steer a single beam carrying modulated signals without degrading the system performance.

2. Layout and key functionalities of the integrated OBFN-PIC

Fig. 1. (b) presents the functional layout of the OBFN-PIC. It comprises of four building blocks, each performing a specific function. The first one is the splitting stage, where the unmodulated optical carrier enters through the fiber array A (FA.A) and split into 8 copy signals by an array of cascaded Mach-Zehnder interferometers (MZIs). Four of these signals are coupled to the next stage which performs the modulation. It consists of four InP phase modulators (PMs) that are driven by microwave signals. After modulation, two sidebands accompany the carrier on either side with frequency difference equal to the central frequency of the microwave signal. Subsequently, the modulated signals are coupled back to the TriPleX® platform and enter to the 4x4 Blass-matrix-based OBFN. The OBFN consists of four waveguide columns and rows, interconnected by a means of a tunable MZI equipped with an additional phase shifter at its output port. All phase shifters are heater-based. The OBFN is dynamically configured based on the evaluated use-case [7]. The processed signals along with the four unmodulated optical carriers from the first stage are coupled to the last stage which involves optical filtering, implemented as asymmetric ring assisted Mach-Zehnder interferometer (RAMZI) [2]. The filters suppress both the optical carrier and one sideband of the modulated signals (SSB-SC filters), while simultaneously re-inserting the optical carrier from the first stage. Finally, the signals are inserted to the FA.C and detected by external photodiodes. In this experimental evaluation, we focus on the performance of the Blass-matrix OBFN. To simplify the assessment and decouple the performance of the integrated modulators, we bypassed the on-PIC modulation stage and used instead an external phase modulator.

3. Experimental set-up and results

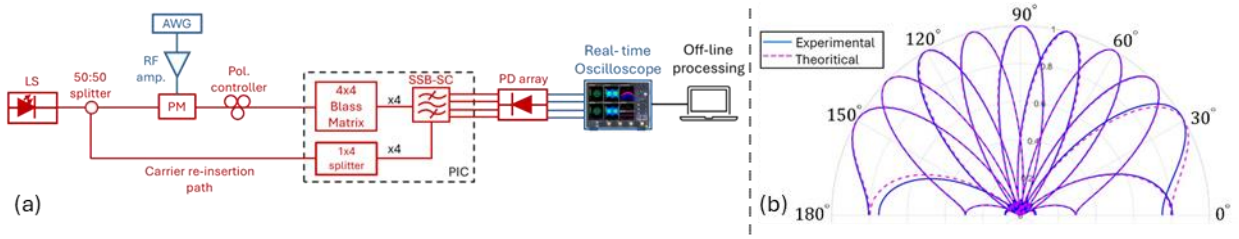

Fig. 2. (a) Schematic of the experimental set-up. (b) Theoretical (dotted line) and experimental (solid line) array factors for operation with sine waves at 12 GHz and beam angles from 30° to 150° with 15° step.

The beamforming capabilities of the OBFN-PIC are demonstrated by simulating a wireless communication system operating in the downlink direction. Fig. 2. (a) presents the experimental setup for its performance assessment. It consists of the OBFN-PIC (shown in the dotted rectangle) along with commercially available passive optics, optoelectronics devices and test and measurement equipment. An external laser source generates an optical carrier at 1568.4 nm with 14 dBm power. The carrier is then split equally into two copy signals using a 50:50 optical splitter. One of them is coupled to an InP phase modulator (PM). The microwave signals driving the PM are generated by a 65 GSa/s arbitrary waveform generator (AWG) producing QPSK modulated signals, after amplification by a low noise amplifier. Several use cases have been evaluated, setting the carrier frequency to 10 and 12 GHz and the symbol rates to 0.25, 0.5 and 1 Gbaud. In each case, the effective bandwidth of the microwave signals is limited using a raised cosine pulse shaping filter with a roll-off factor of 1. A polarization controller and polarization-maintaining fiber are employed to couple the modulated signal and unmodulated carrier to the OBFN-PIC, respectively, with the proper polarization. The modulated signal is directly coupled to $MZI_{4.1}$ through FA.D as shown in Fig. 1. (b). From there, it is routed to $MZI_{4.4}$ by setting the MZIs in between to cross-state. Subsequently, the signal is evenly split into four outputs by the MZIs of the fourth column and each of them is individually processed by the corresponding phase shifters following the MZIs. For every beam use case, from 30° to 150° beam angles, the relative phases were dynamically configured based on the above equation:

$$\Delta\varphi = k_{RF} d \cos(\theta_0) \quad (1)$$

where k_{RF} is the wavenumber, d is the spacing between successive antenna elements, always set at $\lambda_{RF}/2$, and θ_0 is the targeted beam angle [9]. On the other hand, the unmodulated optical carrier is coupled to the OBFN-PIC through the FA.A, as shown also in Fig. 1. (b). The carrier is split into four signals which are routed to the four filters and combined with the modulated optical signals. Filter outputs are then coupled to the FA.C and subsequently, are

detected by a quad array of photodiodes with 3-dB bandwidth equal to 12 GHz. The generated electrical signals are sampled by a 4-channel real-time oscilloscope with 33 GHz analog bandwidth and 80 GSa/s sampling rate. After offline processing the radiated field is calculated, assuming transmission from a linear 4-element antenna array with λ/2 spacing. The results shown in Fig. 2. (b) well agree with the theoretical beam patterns. A receiving antenna placed at a specific beam angle detects the radiated field. The detected microwave signal is down-converted to baseband using a digital local oscillator, and the in-phase and quadrature components are analyzed. A low-pass filter is applied to eliminate unwanted spectral content and standard digital signal processing (DSP) algorithms are utilized for signal decoding and quality assessment, including amplitude level correction, timing recovery, and carrier phase recovery. Finally, constellation diagrams and EVMs are calculated to evaluate the beamforming performance.

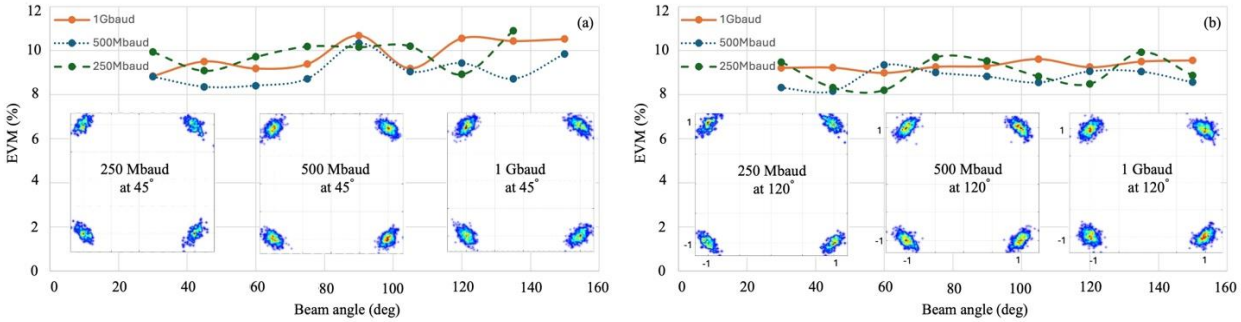

Fig. 3. EVMs for each experimental case at (a) 10 GHz and (b) 12 GHz central frequencies. As insets are shown the reconstructed indicative constellation diagrams at (a) 45° and (b) 120° beam angles.

Fig. 3 presents the EVM values of the detected signals at the output of the DSP algorithms. As indicative examples, the constellation diagrams at 45° and 120° beam angles at 10 and 12 GHz are shown as insets, respectively. An error free performance has been achieved for all the use cases, validating the operation of the OBFN-PIC to form and steer the microwave beams at both central frequencies and symbol rates from 250 Mbaud to 1 Gbaud for all the considered beam angles. The deviation of the EVM values for each use case is lower than 1.1%. The residual phase noise, represented as tangential noise in the constellation diagrams, arises because the optical carrier is split off-PIC and each copy signal (modulated and unmodulated) follows optical paths of unequal lengths. It is expected that by utilizing the on-PIC optical modulators, the impact of the phase noise will be suppressed.

4. Conclusion

We have reported on the system evaluation of a 4x4 Blass-matrix-based OBFN integrated on a silicon-nitride platform. Utilizing 0.25, 0.5 and 1 Gbaud QPSK signals at 10 and 12 GHz and an experimental setup that emulates the operation of the OBFN-PIC in the downlink direction of a wireless communication system, we have evaluated the EVM performance of the decoded signals for beam angles ranging from 30° to 150°. In all cases, error-free performance has been successfully achieved, validating the capability to form and steer a single beam carrying modulated microwave signals without deteriorating the overall system performance.

5. Acknowledgements

This work has received funding from the EU Horizon Europe projects TERA6G (Grant agreement ID:101096949), POLYNICES (Grant agreement ID:101070549) and SPRINTER (Grant agreement ID:101070581).

6. References

[1] Dietze, K. et al. (2000) ‘Smart antennas in wireless communications: Base-Station Diversity and handset beamforming’, IEEE Antennas and Propagation Magazine, 42(5), pp. 142–151.
[2] Berger, P. et al. (2011) ‘Time delay generation at high frequency using SOA based slow and fast light’, Optics Express, 19(22), p. 21180.
[3] Tsokos, C. et al. (2021) ‘True time delay optical beamforming network based on hybrid INP-silicon nitride integration’, 39(18), pp. 5845–5854.
[4] Camponeschi, F. et al. (2024) ‘Multibeam beamforming demonstration of a hybrid integrated photonic module for a synthetic aperture radar receiver’, JLT, pp. 1–8.
[5] D. Madrid at al., “A novel 2N beams heterodyne optical beamforming architecture based on N×N optical Butler matrices”, 2002 IEEE MTT-S International Microwave Symposium Digest.
[6] C. Roeloffzen, et al., "Integrated Optical Beamformers", *Optical Fiber Communication Conference*, 2015.
[7] Tsokos, C. et al. (2018) ‘Analysis of a multibeam optical beamforming network based on Blass Matrix Architecture’, JLT, 36(16), pp. 3354–3372.
[8] Santacruz, J.P. et al. (2023) ‘Incoherent optical beamformer for AROF Fronthaul in MM-wave 5G/6G Networks’, JLT, 41(5), pp. 1325–1334.
[9] R. Mailloux, Phased Array Antenna Handbook (Artech House antennas and propagation library). Artech House, 2005.